Resonant-line overlap for photopumping and spoiling of x-ray lasing transitions in neonlike Fe XVII and Cu XX

P. Beiersdorfer, S. R. Elliott, and J. Nilsen
Lawrence Livermore National Laboratory, Livermore, California 94550
(Received 25 August 1993)

High-precision measurements (25–175 ppm) have been performed of selected $2p$-$3s$ and $2p$-$4d$ transitions in neonlike Fe and Cu that are of possible use in resonant photopumping x-ray lasing experiments. A marginal resonance of 600 ppm is found for the $2p$-$4d$ transition in neonlike Fe with the $1s$-$2p$ transition in hydrogenic Ne. By contrast, an excellent resonance of 200 ppm is determined for photopumping of the $2p$-$4d$ transition in neonlike Cu with the $1s$-$2p$ transition in heliumlike Mg, suggesting that the Cu-Mg pair is a good candidate for resonant photopumping experiments. Moreover, the separation of the $2p$-$3s$ transition in neonlike Fe and the $1s$-$2p$ transition in heliumlike F is measured to assess the resonance for use in a scheme to spoil x-ray lasing. The overlap (2000 ppm), however, appears insufficient.

PACS number(s): 42.60.By, 32.30.Rj, 42.55.Vc

I. INTRODUCTION

X-ray lasing has been observed in neonlike ions ranging from Ti to Ag [1–7]. In these experiments, inversion between the $2p^53p$ upper and the $2p^53s$ lower levels is accomplished by collisional excitation of the closed-shell neonlike ground state $1s^22s^22p^6$. Resonant photopumping has been proposed as an alternate way to achieve lasing [8]. It offers the advantage of higher efficiency in situations where the pump line can be produced efficiently. One example is pulse power machines where it is possible to concentrate as much as 10% of the drive energy in candidate pump lines [9]. Resonant photopumping also has the potential for improving the efficiency of existing lasing schemes and producing lasing on different transitions than those driven in collisional or recombination lasing schemes. However, while resonant photoexcitation of x-ray transitions was demonstrated in fluorescence experiments [10], photopumped x-ray lasing has not yet been observed experimentally. A major drawback of the resonant photopumping scheme is the need to generate a sufficiently high photon density in the pump that can effectively compete with collisional processes. For example, in experiments to attain photopumping of neonlike Rb ($Z=37$) by nickel-like Pt ($Z=78$) or nickel-like Au ($Z=79$), lasing has not been observed because the electron temperature required to generate sufficient photon flux in the Pt or Au pump lines could not be achieved [11]. The lack of success occurred despite the very close resonance between the lines in the pump and lasant ions [12].

In the following we report a measurement of the resonance between neonlike Fe ($Z=26$) and the Ly-α line in hydrogenic Ne ($Z=10$), as well as between neonlike Cu ($Z=29$) and the $1\,^1S_0$–$2\,^3P_1$ intercombination line in heliumlike Mg ($Z=12$). Because of the relatively low atomic number of the ions involved, the necessary pump strength could be achieved much more easily than in experiments involving higher-Z ions, such as nickel-like Au. Thus the Fe-Ne and Cu-Mg schemes are experimentally very attractive. Theoretical investigations of lasing based on these two combinations were published recently, and gains of 2–4 cm^{-1} were predicted [9,13]. The present work thus extends earlier measurements of candidate pairs for resonant photopumping of highly charged high-Z ions [12,14] to ions of lower atomic number, complementing the measurements of heliumlike and hydrogenic ions from Al through K reported recently [15].

We also present a measurement of a photoresonance between one of two $2p^53s$ dump levels in neonlike Fe and the $1\,^1S_0$–$2\,^1P_1$ resonance line in heliumlike F. In principle, this resonance could be used to spoil lasing by resonantly populating the lower neonlike lasing level and reducing or eliminating a population inversion. Demonstrating spoiling by a photoresonance would provide insights into the mechanisms of x-ray lasing. However, we find an inadequate overlap.

II. THEORY

A diagram showing the levels involved in the Fe-Ne resonant photopumping scheme is shown in Fig. 1. The Ly-α pump line in hydrogenic Ne resonates with and pumps the $2p_{1/2}$-$4d_{3/2}$ transition in neonlike Fe. The

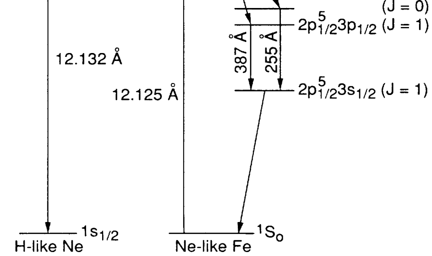

FIG. 1. Energy-level diagram showing the mechanism for resonant photopumping of neonlike Fe by hydrogenlike Ne. Photopumping of the $2p_{1/2}$-$4d_{3/2}$ transition in neonlike Fe feeds an inversion between the $3s$ and $3p$ levels.

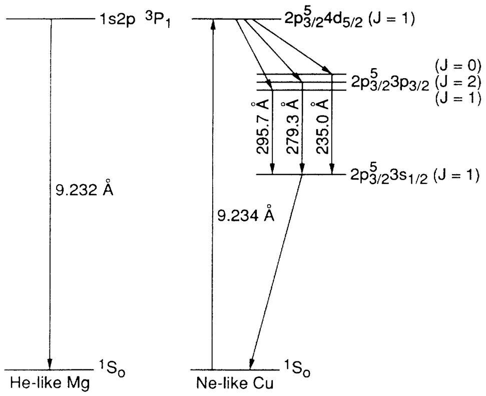

FIG. 2. Energy-level diagram showing the mechanism for resonant photopumping of neonlike Cu by heliumlike Mg. Photopumping of the $2p_{3/2}$-$4d_{5/2}$ transition in neonlike Cu feeds an inversion between the $3s$ and $3p$ levels.

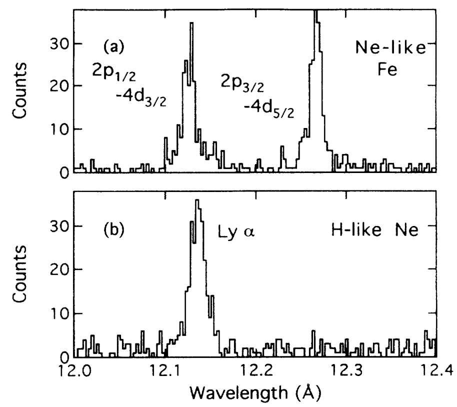

FIG. 4. Crystal-spectrometer spectra of (a) $2p$-$4d$ transitions in neonlike Fe and (b) $1s$-$2p$ transitions in hydrogenlike Ne.

$(2p^5_{1/2}4d_{3/2})_{J=1}$ level predominantly decays to the $(2p^5_{1/2}3p_{1/2})_{J=0}$ and $(2p^5_{1/2}3p_{1/2})_{J=1}$ levels. This establishes an inversion with the $(2p^5_{1/2}3s_{1/2})_{J=1}$ level and may result in lasing among several $3p \rightarrow 3s$ transitions, primarily at 255 and 387 Å [9]. The $(2p^5_{1/2}3s_{1/2})_{J=1}$ level then decays quickly to the $^1S_0$ neonlike ground state.

The photo-pumping scheme for the Cu-Mg laser is shown in Fig. 2. Here the $1\,^1S_0-2\,^3P_1$ intercombination line in heliumlike Mg pumps the $2p_{3/2}$-$4d_{5/2}$ transitions in neonlike Cu. The $(2p^5_{3/2}4d_{5/2})_{J=1}$ level decays preferentially to the $(2p^5_{3/2}3p_{3/2})_{J=0,1,2}$ levels as well as to the $(2p^5_{3/2}3p_{1/2})_{J=1,2}$ levels. Again, this causes an inversion and is predicted [13] to result in lasing among several $3p \rightarrow 3s$ transitions. The largest gain is predicted for the transition $(2p^5_{3/2}3p_{3/2})_{J=1} \rightarrow (2p^5_{3/2}3s_{1/2})_{J=1}$ at 296 Å, which recently has been seen to lase in collisionally pumped neonlike Cu experiments [16].

Photopumping may not only enhance or produce lasing; it may also spoil an inversion and prevent lasing. In particular, lasing can be spoiled by resonantly pumping the lower lasing level and raising its population to the point where there is an insufficient inversion among the $2p^53s$ and $2p^53p$ levels. Figure 3 illustrates this process. The $1\,^1S_0-2\,^1P_1$ resonance line in heliumlike F pumps the $2p_{1/2}$-$3s_{1/2}$ transition in neonlike Fe at 16.772 Å. This enhances the population of the $(2p^5_{1/2}3s_{1/2})_{J=1}$ level, which is the lower level for several $3p \rightarrow 3s$ lasing transitions (cf. Fig. 1), including several lasing transitions that are pumped collisionally. In recent experiments, the 255-Å lasing line was observed to dominate lasing in neonlike Fe together with a weaker 348-Å line [17]. In this case, photopumping could be applied to collisionally pumped lasers to destroy the inversion on the strongest laser line. While spoiling is undesirable, it could nevertheless provide valuable insights into the laser kinetics.

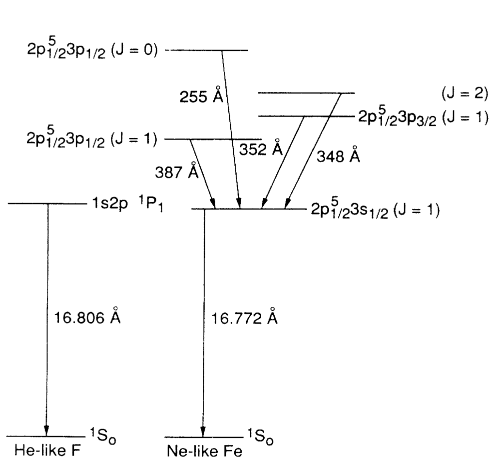

FIG. 3. Energy-level diagram drawing the mechanism for spoiling of lasing in neonlike Fe by resonant photopumping of the $2p_{1/2}$-$3s_{1/2}$ transition by the $1\,^1S_0-2\,^1P_1$ transition in heliumlike F. Increasing the population of the $3s$ level spoils a possible inversion and thus lasing between the $3s$ and $3p$ levels.

III. EXPERIMENT

Measurements are carried out on the Livermore electron-beam ion trap (EBIT) [18] using an evacuated flat-crystal spectrometer [19]. X rays are analyzed either by a 2.5×5-cm^2 mica crystal or by a 2.0×5-cm^2 cesium hydrogen phthalate (CsAP) crystal. The resolving power of the crystals and the detector limit the spectral resolution to $\lambda/\Delta\lambda=500$ for the Fe-F measurements (first-

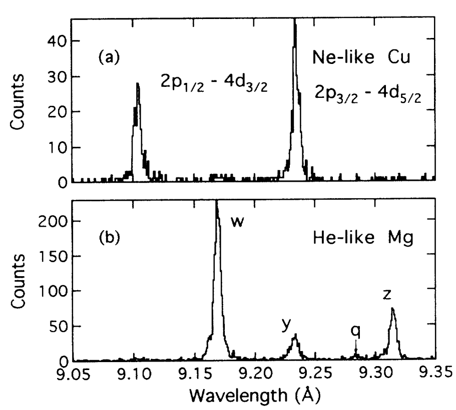

FIG. 5. Crystal-spectrometer spectra of (a) $2p$-$4d$ transitions in neonlike Cu and (b) K-shell transitions in heliumlike Mg.

order Bragg reflection CsAP), $\lambda/\Delta\lambda=1100$ for the Fe-Ne measurements (first-order Bragg reflection mica), and $\lambda/\Delta\lambda=1200$ for the Cu measurements (second-order Bragg reflection CsAP).

Spectra of the $2p$-$4d$ transition in neonlike Fe and the $1s$-$2p$ Ly-α transition in hydrogenic Ne are shown in Fig. 4. Besides the $(2p^5_{1/2}4d_{3/2})_{J=1}\to(2p^6)_{J=0}$ transition of interest to the photopumping scheme, we also observe the neighboring $(2p^5_{3/2}4d_{5/2})_{J=1}\to(2p^6)_{J=0}$ transition. The Ly-α transition is a composite of the transitions $2p_{3/2}\to1s_{1/2}$ and $2p_{1/2}\to1s_{1/2}$. To calibrate the spectra we set the wavelength of the Ly-α feature to 12.1339 Å, which is an intensity-weighted average of the individual transitions calculated by Johnson and Soff [20]. The dispersion is determined from the 11.7-eV splitting of the two $2p$-$4d$ transitions calculated with the code of Grant *et al.* [21]. Although the value of the splitting is estimated to be accurate only within 0.5 eV, this uncertainty only negligibly (≤0.03 eV) reduces the accuracy with which we can determine the separation of the Ne Ly-α and the Fe $2p_{1/2}$-$4d_{3/2}$ transition. In particular, the hydrogenic $1s_{1/2}$-$2p_{3/2}$ and neonlike $2p_{1/2}$-$4d_{3/2}$ transitions are found to be 0.57 ± 0.10 eV apart, or 600 ppm, whereby the uncertainty is dominated by the statistics. For conversion between wavelength and energy we used $hc=12\,398.42$ eV Å [22].

Spectra of the $2p$-$4d$ transitions in neonlike Cu and the K-shell transitions in heliumlike Mg are shown in Fig. 5. Again, the $2p_{1/2}$-$4d_{3/2}$ and $2p_{3/2}$-$4d_{5/2}$ transitions can be identified in the Cu spectrum. The Mg K-shell spectrum shows three heliumlike features, the $1s2p\ ^1P_1\to1s^2\ ^1S_0$ resonance transition w, the $1s2p\ ^3P_1\to1s^2\ ^1S_0$ intercombination line y, and the $1s2s\ ^3S_1\to1s^2\ ^1S_0$ forbidden line z. A fourth line commonly seen in the K-shell spectra of higher-Z heliumlike ions [23], the $1s2p\ ^3P_2\to1s^2\ ^1S_0$ transition labeled x, can only be identified by least-squares fitting procedures on the high-energy side of y. The spectrum also shows a line from lithiumlike Mg, the transition $1s2s2p\ ^2P_{3/2}\to1s^22s\ ^2S_{1/2}$, labeled q, which is the strongest among the lithiumlike K-shell transitions. To calibrate the spectra we set the wavelength of w and z to 9.1688 and 9.3143 Å, respectively, as calculated by Drake [24]. Doing so gives both an absolute scale and the dispersion. The separation of the Cu $2p_{3/2}$-$4d_{5/2}$ and the Mg intercombination line is measured to be 0.27 ± 0.10 eV or 200 ppm. Again, the uncertainty in the measurement is dominated by statistics. The measured energy of y is 1342.96 ± 0.10 eV. This is slightly less than Drake's value of 1343.10 eV. The discrepancy does not affect the measured separation. In other words, if we used Drake's value for y for calibration, the measured value for the Cu $2p_{3/2}$-$4d_{5/2}$ would be 0.14 eV larger, but the separation would still be 0.27 ± 0.10 eV.

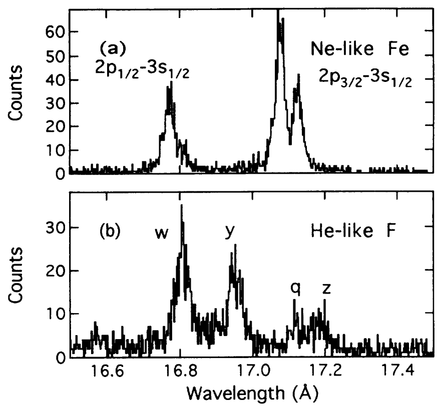

FIG. 6. Crystal-spectrometer spectra of (a) $2p$-$3s$ transitions in neonlike Fe and (b) K-shell transitions in heliumlike F. The Fe spectrum shows both the $(2p_{1/2}$-$3s_{1/2})_{J=1}$ and the $(2p_{3/2}$-$3s_{1/2})_{J=1}$ electric-dipole transitions; the third (and longest-wavelength) transition corresponds to the $(2p_{3/2}$-$3s_{1/2})_{J=2}$ magnetic-quadrupole transition.

We note that the low intensity of y measured in our experiment is not an accurate reflection of its intensity under the high-electron density plasma conditions required to make a laser. Unlike in EBIT, where the electron density does not exceed 5×10^{12} cm^{-3}, in a high-density plasma the population of the $^3P_1$ level is drastically enhanced by collisional transfer from other $n=2$ levels, making it nearly equal to the intensity of w [25].

Spectra of the $2p$-$3s$ neonlike transition and the K-shell transitions in heliumlike F are shown in Fig. 6. The Fe spectrum shows not only the $(2p^5_{1/2}3s_{1/2})_{J=1}\to(2p^6)_{J=0}$ transition at 16.772 Å but also the two $(2p^5_{3/2}3s_{1/2})_{J=1,2}\to(2p^6)_{J=0}$ transitions. The $(2p^5_{3/2}3s_{1/2})_{J=2}\to(2p^6)_{J=0}$ magnetic-quadrupole transition is the longest-wavelength transition in the neonlike x-ray spectrum, and because of its small radiative rate can only be observed in low-density plasmas. The spectrum of heliumlike F shows the same features as that of heliumlike Mg in Fig. 5. We note, however, that line y blends with a line from background ions indigenous to EBIT, and the feature seen does not give a true reflection of its intensity. Like the Mg-Cu measurements we calibrate the F-Fe measurements by setting wavelengths of the w and z to the values calculated by Drake [24], i.e., to 16.8064 and 17.1528 Å, respectively. We determine a separation of 1.52 ± 0.16 eV between w and the Fe $2p_{1/2}$-$3s_{1/2}$ line.

TABLE I. Measured transition energies in neonlike Fe and Cu and separation from their respective heliumlike or hydrogenic pump lines. The uncertainty in the last digit(s) is indicated in parentheses.

Neonlike transition	Element	Energy (eV)	Pump transition	Element	Energy (eV)	Separation (eV)
$2p_{1/2}$-$3s_{1/2}$	Fe	739.24(13)	$1\,^1S_0$-$2\,^1P_1$	F	737.72[a]	+1.52(16)
$2p_{1/2}$-$4d_{3/2}$	Fe	1022.52(7)	$1s_{1/2}$-$2p_{3/2}$	Ne	1021.95[b]	+0.57(10)
$2p_{3/2}$-$4d_{5/2}$	Cu	1342.69(3)	$1\,^1S_0$-$2\,^3P_1$	Mg	1342.96(10)	−0.27(10)

[a]Theoretical value from Drake [24].
[b]Theoretical value from Johnson and Soff [20].

An overview of the measured wavelengths, including the heliumlike pump lines and the measured separations, is given in Table I.

IV. CONCLUSION

We have measured the wavelengths of the $2p$-$4d$ and $2p$-$3s$ transitions in neonlike Fe with an accuracy of 0.07 eV. The overlap of the Fe $2p$-$4d$ transitions with the Ne Ly-α line is 0.57 ± 0.10 eV or 600 ppm. The thermal Doppler motion in a 500-eV plasma will broaden the Fe line by 0.2 eV and the Ne line by 0.4 eV. The resonance thus is marginal unless there is significant broadening due to other effects such as opacity broadening. The separation of the Fe $2p$-$3s$ and the F w like is even larger and does not promise any chance of successful resonant pumping.

We have also measured the wavelength of the $2p$-$4d$ transition in neonlike copper with an accuracy of 0.03 eV. We find that the separation of the Cu $2p$-$4d$ and the Mg intercombination line is only 0.27 ± 0.10 eV or 200 ppm. Thermal Doppler motion in a 500-eV plasma will broaden the Cu line by 0.3 eV and the Mg line by 0.5 eV. The resonance condition necessary for successful photopumping thus is satisfied. Moreover, the ionization potentials of Cu and Mg are such that the respective neonlike and heliumlike charge states can coexist in a plasma. Collisional pumping of a neonlike Cu laser has already been demonstrated [2,16], and photopumping of a neonlike Cu laser by Mg appears possibly just as likely to succeed.

ACKNOWLEDGMENTS

We are grateful for the encouragement of M. Eckart, A. Hazi, and S. Libby. We thank A. Faenov for providing us with the CsAP crystal used in the experiment. This work was performed under the auspices of the U.S. Department of Energy by Lawrence Livermore National Laboratory under Contract No. W-7405-ENG-48.

[1] D. L. Matthews *et al.*, Phys. Rev. Lett. **54**, 110 (1985).
[2] T. N. Lee, E. A. McLean, and R. C. Elton, Phys. Rev. Lett. **59**, 1185 (1987).
[3] B. J. MacGowan *et al.*, J. Appl. Phys. **61**, 5243 (1987).
[4] C. J. Keane *et al.*, Phys. Rev. A **42**, 2327 (1990).
[5] D. Naccache *et al.*, Phys. Rev. A **42**, 3027 (1990).
[6] T. Boehly *et al.*, Phys. Rev. A **42**, 6962 (1990).
[7] D. J. Fields *et al.*, Phys. Rev. A **46**, 1606 (1992).
[8] A. V. Vinogradov, I. I. Sobelman, and E. A. Yukov, Sov. J. Quantum Electron. **59**, 5 (1975); B. A. Norton and N. J. Peacock, J. Phys. B **8**, 989 (1975).
[9] J. Nilsen, J. Quantum Spectrosc. Radiat. Transfer **46**, 547 (1991).
[10] P. Monier, C. Chenais-Popovics, J. P. Geindre, and J. C. Gauthier, Phys. Rev. A **38**, 2508 (1988); C. A. Back, C. Chenais-Popovics, and R. W. Lee, *ibid.* **44**, 6730 (1991).
[11] J. Nilsen *et al.*, in *X-Ray Lasers 1992,* edited by E. E. Fill, IOP Conf. Proc. No. 125 (Institute of Physics, Bristol, 1992), p. 137.
[12] S. Elliott, P. Beiersdorfer, and J. Nilsen, Phys. Rev. A **47**, 1403 (1993).
[13] J. Nilsen, Opt. Commun. **78**, 51 (1990).
[14] P. Beiersdorfer *et al.*, Phys. Rev. A **46**, R25 (1992); J. Nilsen, P. Beiersdorfer, and S. R. Elliott, Phys. Scr. **47**, 42 (1993).
[15] K. Gäbel, Ch. Bermann, E. Fill, E. Förster, and I. Uschmann, Appl. Phys. B **56**, 3 (1993).
[16] J. Nilsen, J. C. Moreno, B. J. MacGowan, and J. A. Koch, Appl. Phys. B **57**, 309 (1993).
[17] J. Nilsen, B. J. MacGowan, L. B. DaSilva, and J. C. Moreno, Phys. Rev. A **48**, 4682 (1993).
[18] R. E. Marrs, M. A. Levine, D. A. Knapp, and J. R. Henderson, Phys. Rev. Lett. **60**, 1715 (1988); M. A. Levine *et al.*, Nucl. Instrum. Methods B **43**, 431 (1989).
[19] P. Beiersdorfer and B. J. Wargelin, Rev. Sci. Instrum. **65**, 13 (1994).
[20] W. R. Johnson and G. Soff, At. Data Nucl. Data Tables **33**, 405 (1985).
[21] I. P. Grant, B. J. McKenzie, P. H. Norrington, D. F. Mayers, and N. C. Pyper, Comput. Phys. Commun. **21**, 27 (1980).
[22] E. R. Cohen and B. N. Taylor, Rev. Mod. Phys. **59**, 1121 (1986).
[23] TFR Group, M. Cornille, J. Dubau, and M. Loulergue, Phys. Rev. A **32**, 3000 (1985); R. Zasadzinski, P. Beiersdorfer, D. A. Vogel, and K. Wong, University of California Report No. UCRL-JC-113885, 1993 (unpublished).
[24] G. W. F. Drake, Can. J. Phys. **66**, 586 (1988).
[25] J. L. Porter *et al.*, Phys. Rev. Lett. **68**, 796 (1992).